



## Editor's Choice

Enhancing mechanical toughness of aluminum surfaces by nano-boron implantation: An *ab initio* studyZhen Zhu<sup>a</sup>, Dae-Gyeon Kwon<sup>b</sup>, Young-Kyun Kwon<sup>b</sup>, David Tománek<sup>a,\*</sup><sup>a</sup> Physics and Astronomy Department, Michigan State University, East Lansing, MI 48824, USA<sup>b</sup> Department of Physics and Research Institute for Basic Sciences, Kyung Hee University, Seoul 130-701, Republic of Korea

## ARTICLE INFO

## Article history:

Received 23 October 2014

In final form 28 November 2014

Available online 12 December 2014

## ABSTRACT

Searching for ways to enhance surface hardness of aluminum, we study the equilibrium structure, stability, elastic properties and formation dynamics of a boron-enriched surface using *ab initio* density functional calculations. We used molecular dynamics simulations to model the implantation of energetic boron nanoparticles in Al and identify structural arrangements that optimize the formation of strong covalent B–Al bonds. Nano-indentation simulations based on constrained optimization suggest that presence of boron nanostructures in the subsurface region enhances significantly the mechanical hardness of aluminum surfaces.

© 2014 Elsevier B.V. All rights reserved.

## 1. Introduction

Aluminum owes its widespread use especially in the aerospace industry to its low gravimetric density, good machinability, and high strength-to-weight ratio [1,2]. Since this metal is rather soft, its low wear resistance poses a serious problem especially in harsh environments. The common way to enhance surface hardness of aluminum is by hard-coat anodizing, an electrolytic passivation process, which forms a brittle surface oxide layer that may chip off. Alternative ways to enhance hardness while maintaining ductility mostly involve bulk modifications, such as changing from Al to the Al/TiB<sub>2</sub> composite [3]. Hard diamond-like carbon coatings do not adhere well to the soft Al surface without adhesion promoters at the interface [4]. An intriguing alternative to carbon involves boron that is nearly as hard as diamond and that may bond more strongly to aluminum, since Al belongs to the boron group in the periodic system. Boron is known for its large flexibility in bonding, forming unusual structures in the bulk [5] and in nanoparticles [6]. The ability of boron to harden surfaces of metals including Al has been suggested by the observed increase in their abrasion resistance following bombardment by boron nanoparticles [7].

Here we study the possibility of enhancing the surface hardness of Al by implantation of boron nanoparticles using *ab initio* density functional calculations. Our results include the equilibrium structure, stability, elastic properties and formation dynamics

of a boron-enriched Al surface after exposure to energetic boron nanoparticles. Combining molecular dynamics simulations with structure optimization studies, we identify structural arrangements that optimize the formation of strong covalent B–Al bonds. Nano-indentation simulations based on constrained optimization suggest that presence of boron aggregates enhances significantly the mechanical hardness and wear-resistance of aluminum surfaces.

## 2. Computational methods

Our calculations are based on the *ab initio* density functional theory (DFT) as implemented in the SIESTA code [8]. We used the Ceperley-Alder [9] exchange-correlation functional as parameterized by Perdew and Zunger [10] and norm-conserving Troullier-Martins pseudopotentials [11]. Our basis consisted of pseudo-atomic orbitals (PAOs) generated by the split-valence scheme for a double- $\zeta$  polarized basis set. All calculations were performed using periodic boundary conditions. The (111) surface of aluminum was represented by a five-layer slab, shown in Figure 1(a), with each layer containing four Al atoms per unit cell and the slabs separated by a vacuum region of 10 Å. We sampled the small quasi-2D Brillouin zone associated with the large supercells by a dense  $8 \times 8 \times 1$  *k*-point mesh [12]. The energy shift due to the spatial confinement of the PAO basis functions [13,14] was limited to less than 10 meV. The charge density has been determined self-consistently on a real space mesh with a very high cutoff energy of 180 Ry, sufficient for total energy convergence to within 1 meV/atom. We studied bombardment of Al(111) by boron

\* Corresponding author.

E-mail address: [tomanek@pa.msu.edu](mailto:tomanek@pa.msu.edu) (D. Tománek).

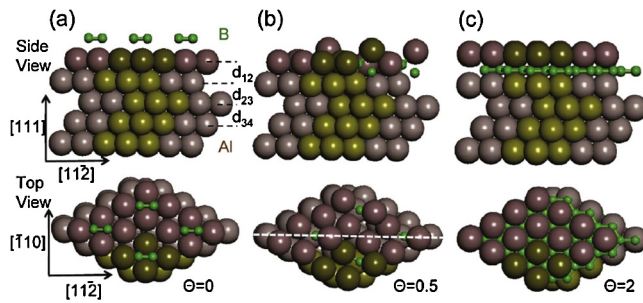


**Figure 1.** Optimized structure of pristine and B enriched Al(111) surfaces in side view (top panels) and top view (bottom panels). (a) Pristine Al(111) surface prior to bombardment by boron dimers, shown above the surface. The most stable structure of the Al surface enriched with (b) 2 B atoms and (c) 8 B atoms per unit cell containing 20 Al atoms. The unit cells used in the study are highlighted by color and shading. (For interpretation of the references to color in this figure legend, the reader is referred to the web version of this article.)

nanostructures using microcanonical molecular dynamics (MD) calculations. We integrated the equations of motion with the Verlet algorithm, using  $\Delta t = 0.5$  fs as time step to cover very long simulation periods of up to 2 ps. The geometry of selected structures was optimized using the conjugate gradient method. A structure was considered optimized when none of the residual forces exceeded 0.01 eV/Å.

### 3. Results and discussion

The key objective of our study is to identify unusually stable, covalently bonded B-Al nanostructures in the surface region of Al following implantation of boron nanoparticles, which would improve wear resistance of Al. Correct description of bonding changes requires treatment by a self-consistent electronic structure calculation. This approach is computationally very demanding and, when combined with molecular dynamics simulations, poses a serious limit on the number of atoms per unit cell. Also, we will represent boron nanoparticles by  $B_2$  molecules when addressing implantation. Our focus will be to investigate favorable bonding changes in specific structural arrangements, which has been neglected in previous studies. Without obtaining this microscopic information, we will not be able to provide an adequate description of compressive strain changes at the surface, the classic mechanism for improving hardness, toughness, and wear at a metal surface.

Before studying implantation of boron nanoparticles, we optimized the structure of the Al(111) surface. We found that slabs with at least five Al layers are required to reproducibly represent the surface relaxation of the topmost layers. To adjust the interface to the optimum bulk structure, the bottom two layers have been constrained in the bulk geometry. In the optimum geometry, shown in Figure 1(a), the largest change in the interlayer separation  $d_{i,i+1}$  occurs for the topmost layer  $i=1$  and decreases with increasing depth below the surface as  $\Delta d_{12}/d_{12} = +2.1\%$ ,  $\Delta d_{23}/d_{23} = +1.2\%$ , and  $\Delta d_{34}/d_{34} = +1.2\%$ . Whereas the topmost layer contracts at most metal surfaces [15], we find a surface expansion in slabs with more than 3 layers in agreement with experimental observation [16], indicating that the close-packed Al(111) surface does not benefit from Smoluchowski smoothing [17].

Next, we need to locate stable atomic arrangements in a boron enriched Al(111) surface that would locally enhance surface hardness. This task is very hard, since there is no empirical guidance for lack of a well-behaved potential energy surface representing boron interacting with aluminum. Global optimization of the positions of 20 Al and additional B atoms in each unit cell, when viewed as a search in configurational space of 60 or more dimensions, appears nearly impossible using DFT due to the high computational

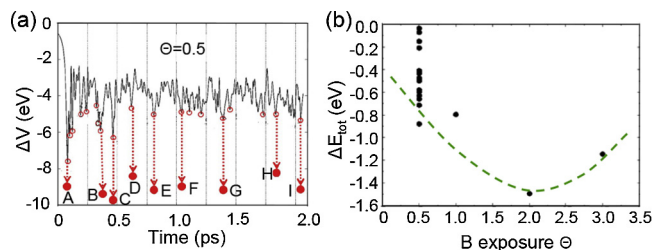


**Figure 2.** Stability of boron enriched Al(111) surfaces. (a) Potential energy evolution during the microcanonical MD simulation of boron dimers impacting on the Al(111) surface. Solid circles below selected potential minima represent optimized structures at  $T=0$  K. (b) Diagram depicting the relative stability change  $\Delta E_{tot}$  of the B enriched Al(111) surface as a function of the B exposure  $\Theta$ . The green dashed line is a guide to the eye. Changes in the potential energy  $\Delta V$  and stability are given per unit cell. (For interpretation of the references to color in this figure legend, the reader is referred to the web version of this article.)

requirements. To represent the experimental conditions, which partly mimic simulated annealing, we first optimized the geometry of the Al(111) surface at  $T=0$  K. Then, we used molecular dynamics simulations to probe structural changes induced by a subsequent impact of energetic boron nanoparticles.

For the sake of simplicity, we limited our MD study to a boron dimer with kinetic energy 0.5 eV/atom that impacted on the surface vertically. A movie of the structural evolution as a function of time, presented in the Supporting Information [18], indicates that the  $B_2$  molecule transfers its excess kinetic energy to locally melt the aluminum surface. Even though the two boron atoms may separate in the hot surrounding Al metal, they eventually remain connected to each other in subsurface sites, as seen in Figure 1(b).

Whereas the total energy is conserved during the molecular dynamics simulation, the continuous transformation between more stable and less stable structures is reflected well in the time-dependence of the potential energy  $V$ , which is presented in Figure 2(a). The time evolution of the system may be viewed as a trajectory in configurational space, and may be compared to the trajectory during a simulated annealing optimization, with potential energy minima representing particularly stable geometries. Since potential energy minima correspond to kinetic energy maxima, high velocity may prevent atoms from probing closely the most stable arrangements. Assuming that minima in the potential energy during our MD simulation are close to optimum atomic arrangements, we froze the corresponding structures and optimized them using the conjugate gradient technique. We believe that these structures, labelled A–I and shown by the solid circles in Figure 2(a), represent some of the most stable geometries of B enriched Al(111). We found that for the most stable among these optimized structures, boron atoms generally occupy interstitial sites below the topmost layer and are connected to each other. This optimum bonding geometry reflects the bond strength hierarchy, with the B–B bonds being the strongest and the B–Al bonds being in-between the B–B and the weakest Al–Al bonds. Thus, the structural priority is to maintain a contiguous optimum B structure that also maximizes bonding to Al, possibly at the expense of disrupting Al–Al bonds. We expect that this can be achieved best by placing boron aggregates below the topmost Al layer. Indeed, we find that structure C in Figure 2(a), which represents the most stable atomic arrangement in the  $B_2Al_{20}$  unit cell and is shown in Figure 1(b), agrees with this stability criterion.

With the above working hypothesis for optimum atomic arrangements at hand, we next discuss ways to enhance the stability of the Al(111) surface by changing the concentration of boron in the surface region. The corresponding results are presented in Figure 2(b), where we define the boron exposure  $\Theta$  by the ratio of the total number of B atoms  $N$  and the

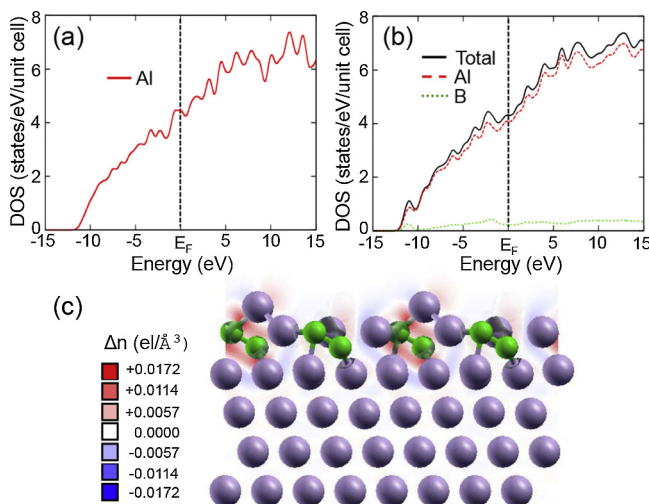


**Figure 3.** Effect of B-Al bonding on the electronic structure. The electronic density of states (DOS) of (a) a pristine Al(111) slab and (b) the slab structure of Figure 1(b) with  $\Theta = 0.5$ . The partial DOS of Al is shown by the dashed line and that of B is shown by the dotted line in (b). (c) Charge density difference in the system of (b), presented as a contour plot in a plane normal to the surface, indicated by the dashed line in Figure 1(b).

number of surface Al atoms  $N_s(\text{Al}) = 4$  in the unit cell of the slab. We next define the stability change associated with the presence of B atoms by the total energy difference per unit cell  $\Delta E_{\text{tot}} = [E_{\text{tot}}(B_N\text{Al}_{20}) - E_{\text{tot}}(\text{Al}_{20}) - NE_{\text{tot}}(B_{\text{ref}})]/N$ . We chose to use  $E_{\text{tot}}(B_{\text{ref}}) = E_{\text{tot}}(B_{12})/12$  as the boron reference energy, since  $B_{12}$  icosahedra are not only very stable as nanoparticles, but also occur as building blocks of the bulk structure of elemental boron [5],  $\alpha$ -B and  $\beta$ -B. Then, the sign of  $\Delta E_{\text{tot}}$  should reflect the energetic preference of boron atoms to either form stable isolated nanoparticles or rather to form nanostructures embedded in the metal matrix. Our results indicate that structures with  $\Theta = 0.5$  are generally less stable than systems with a higher B concentration. Among the systems investigated in our study, we found the  $\Theta = 2.0$  structure depicted in Figure 1(c) to be the most stable. The  $B_8\text{Al}_{20}$  surface compound benefits from the stability of the contiguous planar boron honeycomb lattice sandwiched between the topmost and the second Al layer, which locally resembles the structure of the stable  $\text{AlB}_2$  compound. Considering stability changes per boron atom, as reflected in the definition of  $\Delta E_{\text{tot}}$  above, the  $B_8\text{Al}_{20}$  structure is more stable by 0.6 eV/B atom than the boron poorer  $\text{B}_2\text{Al}_{20}$  and by 0.3 eV/B atom than the boron richer  $B_{12}\text{Al}_{20}$  system.

As suggested in the beginning, the reason for very strong bonding between B and Al is that both elements are in the same group of the periodic system. In this case, we expect only a moderate charge transfer and covalent bonds between neighboring B and Al atoms. Results related to the electronic structure of B enriched Al are presented in Figure 3. The electronic density of states (DOS) of the topmost 2 layers of the Al(111) surface, shown in Figure 3(a), is close to that of a free-electron metal. The corresponding DOS of the topmost 2 layers of the B-enriched Al(111) surface, with the structure depicted in Figure 1(b), is presented in Figure 3(b). Comparing these two densities of states, including the projection onto Al and B sites in Figure 3(b), indicates only a moderate perturbation of the Al subsystem by bonding to boron. Mulliken population results with a single- $\zeta$  basis indicate net transfer of  $\approx 0.7$  electrons from Al to B in the structure of Figure 1(b). To get a more accurate idea about the charge redistribution in the system caused by the presence of B in Al(111), we plotted in Figure 3(c) the electron density difference  $\Delta n(\mathbf{r}) = n_{\text{B}_x\text{Al}_{1-x}}(\mathbf{r}) - n_{\text{Al}}(\mathbf{r}) - n_{\text{B}}(\mathbf{r})$ . Taking  $n_{\text{Al}}(\mathbf{r})$  and  $n_{\text{B}}(\mathbf{r})$  as the electron densities of the isolated, frozen subsystems,  $\Delta n(\mathbf{r})$  is nonzero only in regions, where the total electron density deviates

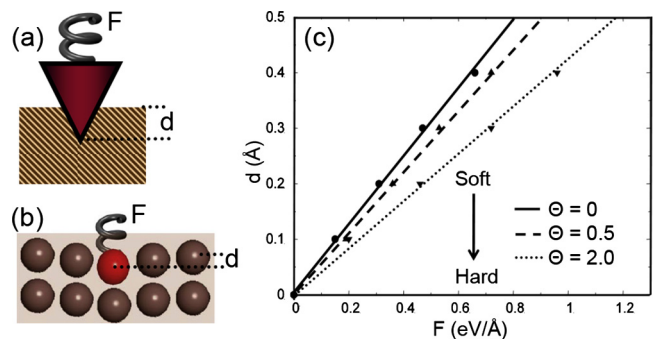


**Figure 4.** Effect of nano-boron on the surface hardness of Al. Schematic model of a Rockwell nano-indenter in (a) is compared to its atomic-scale counterpart in (b). (c) Displacement  $d$  as a function of the force  $F$  pressing vertically on a surface atom in  $\text{B}_x\text{Al}(111)$ . Results are presented for structures with  $\Theta = 0$ ,  $\Theta = 0.5$  and  $\Theta = 2.0$ , depicted in Figure 1(a)–(c).

from a mere superposition of the subsystem charge densities. Our calculated  $\Delta n(\mathbf{r})$  in Figure 3(c) indicates a moderate electron transfer from Al to B, in agreement with the Mulliken analysis, with many Al neighbors of B contributing as electron donors. Close inspection of Figure 3(c) reveals that presence of Al does not change the B–B bond and vice versa. A large electron accumulation in the region of Al–B bonds suggests that Al–B bonds are covalent and should be strong as anticipated.

There is no easy way to provide a realistic description of surface hardness, as probed by nano-indentation, in atomistic calculations, due to the complexity of processes including plastic flow associated with dislocation motion along slip planes in the sample. Instead of explicitly considering large-scale displacement of atoms during indentation, we note that plastic flow is initiated at defects that require particularly low activation barriers for nucleation. It has been shown that such low nucleation barriers are commonly found at defects that form within the anharmonic regime of soft harmonic modes [19]. This correlation provides a direct link between softness in the elastic response and plastic activity. In this case, we should be able to get valuable insight into surface hardness by probing the elastic response only.

In the following, we study this important quantity by replicating the way hardness is probed experimentally using nano-indentation and focussing on the initial elastic response. The schematic setup of the commonly used Rockwell nano-indentation test is shown in Figure 4(a). Rockwell hardness is determined by the indentation depth  $d$  of a hard, conical nano-indenter that is pressed by force  $F$  towards the surface. The deeper the indentation at a given load, the softer the material. As an atomic-scale analogy, we studied structural rearrangements introduced by a vertical displacement of a surface atom by  $d$  with respect to the bottom of the slab, as illustrated schematically in Figure 4(b). For different values of  $d$ , we optimized the position of all atoms in the unit cell except the constrained atom, considered a ‘nano-indenter’, and the bottom of the slab. We then interpreted the vertical component of the Hellmann-Feynman force acting on the nano-indenter as the load  $F$  associated with the indentation  $d$ .

Our results for the atomic nano-indentation process are presented in Figure 4(c) for the three structures shown in Figure 1, representing different degrees of boron enrichment. These results indicate a linear relationship between the load and the indentation depth for  $d$  below 0.5 Å. Defining local surface hardness by the  $F/d$  ratio, we find the values 1.6 eV/Å<sup>2</sup> or 25.6 J/m<sup>2</sup> for pure Al(111) ( $\Theta = 0$ ), 1.8 eV/Å<sup>2</sup> or 28.8 J/m<sup>2</sup> for a low nano-boron exposure  $\Theta = 0.5$  and 2.4 eV/Å<sup>2</sup> or 38.4 J/m<sup>2</sup> for the higher nano-boron exposure  $\Theta = 2.0$ . Considering the fact that the net amount of nano-boron is rather small, the increase of the surface hardness by 13%

for  $\Theta = 0.5$  and by 50% for  $\Theta = 2.0$  is formidable. We must note that our five-layer slab is a very limited representation of a realistic polycrystalline surface, where energetic boron nanoparticles may penetrate deeper, modifying the grain structure and reinforcing intergranular interfaces by covalent bonds. We wish our study to inspire corresponding experiments.

#### 4. Summary and conclusions

In conclusion, we used *ab initio* density functional calculations to study the equilibrium structure, stability, elastic properties and formation dynamics of a boron-enriched Al(111) surface. We used molecular dynamics simulations to model the implantation of energetic boron nanoparticles in Al and identified structural arrangements that optimize the formation of strong covalent B-Al bonds for different concentrations of boron in the surface region. Nano-indentation simulations based on constrained optimization suggest that presence of contiguous boron nanostructures in the subsurface region may increase the mechanical hardness of aluminum surfaces by up to 50% at relatively low boron exposures.

#### Acknowledgments

This study was inspired by the observations of Rick Becker that bombardment by boron nanoparticles improved significantly the wear resistance of metal surfaces. It was supported by the National Science Foundation Cooperative Agreement #EEC-0832785, titled "NSEC: Center for High-rate Nanomanufacturing". Computational resources have been provided by the Michigan State University High Performance Computing Center and the KISTI Supercomputing Center (KSC-2013-C2-024).

#### Appendix A. Supplementary data

Supplementary data associated with this article can be found, in the online version, at <http://dx.doi.org/10.1016/j.cplett.2014.11.070>.

#### References

- [1] W. Miller, L. Zhuang, J. Bottema, A. Wittebrood, P.D. Smet, A. Haszler, A. Vieregge, Recent development in aluminium alloys for the automotive industry, *Mater. Sci. Eng. A* 280 (2000) 37.
- [2] M. Ashby, Y. Bréchet, D. Cebon, L. Salvo, Selection strategies for materials and processes, *Mater. Des.* 25 (2004) 51.
- [3] A.V. Smith, D.D.L. Chung, Titanium diboride particle-reinforced aluminium with high wear resistance, *J. Mater. Sci.* 31 (1996) 5961.
- [4] C. Srivida, S.V. Babu, Corrosion resistance of diamond-like carbon-coated aluminium films, *Chem. Mater.* 8 (1996) 2528.
- [5] M. Widom, M. Mihalkovič, Symmetry-broken crystal structure of elemental boron at low temperature, *Phys. Rev. B* 77 (2008) 064113.
- [6] I. Boustani, Z. Zhu, D. Tománek, Search for the largest two-dimensional aggregates of boron: an *ab initio* study, *Phys. Rev. B* 83 (2011) 193405.
- [7] Rick Becker (private communication).
- [8] E. Artacho, E. Anglada, O. Dieguez, J.D. Gale, A. García, J. Junquera, R.M. Martin, P. Ordejón, J.M. Pruneda, D. Sanchez-Portal, J.M. Soler, The siesta method: developments and applicability, *J. Phys. Condens. Mater.* 20 (2008) 064208.
- [9] D.M. Ceperley, B.J. Alder, Ground state of the electron gas by a stochastic method, *Phys. Rev. Lett.* 45 (1980) 566.
- [10] J.P. Perdew, A. Zunger, Self-interaction correction to density-functional approximations for many-electron systems, *Phys. Rev. B* 23 (1981) 5048.
- [11] N. Troullier, J.L. Martins, Efficient pseudopotentials for plane-wave calculations, *Phys. Rev. B* 43 (1991) 1993.
- [12] H.J. Monkhorst, J.D. Pack, Special points for brillouin-zone integrations, *Phys. Rev. B* 13 (1976) 5188.
- [13] O.F. Sankey, D.J. Niklewski, *Ab initio* multicenter tight-binding model for molecular-dynamics simulations and other applications in covalent system, *Phys. Rev. B* 40 (1989) 3979.
- [14] E. Artacho, D. Sánchez-Portal, P. Ordejón, A. García, J.M. Soler, Linear-scaling *ab initio* calculations for large and complex system, *Phys. Stat. Sol. B* 215 (1999) 809.
- [15] A. Zangwill, *Physics at Surfaces*, Cambridge University Press, Cambridge, UK, 1988.
- [16] D.W. Jepsen, P.M. Marcus, F. Jona, Low-energy-electron diffraction from several surfaces of aluminum, *Phys. Rev. B* 6 (1972) 3684, and *Phys. Rev. B* 8, (1973) 1786(E).
- [17] R. Smoluchowski, Anisotropy of the electronic work function of metals, *Phys. Rev.* 60 (1941) 661.
- [18] See the supporting information for a movie of the molecular dynamics simulation depicting structural changes at the Al(111) surface following impact of B<sub>2</sub> nanoparticles. Different layers of the Al substrate are distinguished by color to visually identify local melting.
- [19] J. Rottler, S.S. Schoenholz, A.J. Liu, Predicting plasticity with soft vibrational modes: from dislocations to glasses, *Phys. Rev. E* 89 (2014) 042304.